

High Energy Emission from the Starburst Galaxy NGC 253

Yoel Rephaeli^{1,2*}, Yinon Arieli¹ and Massimo Persic³

¹*School of Physics and Astronomy, Tel Aviv University, Tel Aviv, 69978, Israel*

²*Center for Astrophysics and Space Sciences, University of California, San Diego, La Jolla, CA 92093-0424*

³*INAF/Osservatorio Astronomico di Trieste and INFN-Trieste, via G.B. Tiepolo 11, 34143 Trieste, Italy*

15 June 2018

ABSTRACT

Measurement sensitivity in the energetic γ -ray region has improved considerably, and is about to increase further in the near future, motivating a detailed calculation of high-energy (HE: ≥ 100 MeV) and very-high-energy (VHE: ≥ 100 GeV) γ -ray emission from the nearby starburst galaxy NGC 253. Adopting the convection-diffusion model for energetic electron and proton propagation, and accounting for all the relevant hadronic and leptonic processes, we determine the steady-state energy distributions of these particles by a detailed numerical treatment. The electron distribution is directly normalized by the measured synchrotron radio emission from the central starburst region; a commonly expected theoretical relation is then used to normalize the proton spectrum in this region. Doing so fully specifies the electron spectrum throughout the galactic disk, and with an assumed spatial profile of the magnetic field, the predicted radio emission from the full disk matches well the observed spectrum, confirming the validity of our treatment. The resulting radiative yields of both particles are calculated; the integrated HE and VHE fluxes from the entire disk are predicted to be $f(\geq 100 \text{ MeV}) \simeq (1.8_{-0.8}^{+1.5}) \times 10^{-8} \text{ cm}^{-2} \text{ s}^{-1}$, and $f(\geq 100 \text{ GeV}) \simeq (3.6_{-1.7}^{+3.4}) \times 10^{-12} \text{ cm}^{-2} \text{ s}^{-1}$, with a central magnetic field value $B_0 \simeq 190 \pm 10 \mu\text{G}$. We discuss the feasibility of measuring emission at these levels with the space-borne *Fermi* and ground-based Cherenkov telescopes.

Key words: galaxies:cosmic rays – galaxies:gamma-ray – galaxies:spiral – galaxies:star formation

1 INTRODUCTION

High star formation (SF) and supernova (SN) rates in starburst (SB) galaxies (SBGs) enhance the energy density of energetic nonthermal particles - mostly electrons and protons - which are accelerated by SN shocks. Coulomb, synchrotron and Compton energy losses by the electrons, and the decay of pions following their production in energetic proton interactions with the ambient gas, result in emission over the full electromagnetic spectrum, from radio to high-energy (HE: ≥ 100 MeV) γ -rays. The relatively high level of emission in SBGs (as compared with emission from ‘normal’ galaxies) suggests nearby SBGs as viable candidates for detection by γ -ray facilities, such as the space-borne *Fermi* telescope, and the imaging air Cherenkov telescopes (IACTs) H.E.S.S., MAGIC, and VERITAS (e.g., De Angelis et al. 2008), all of which have already detected emission from a sample of AGN. When γ -ray emission is detected from SBGs, important additional insight will be gained on the origin and propagation mode of energetic electrons and protons in these galaxies. However, only weak level of emission is expected, making nearby SBGs the obvious choice of our study and potential targets for observations. A realistic estimate of the expected γ -ray emission requires a detailed account of all relevant energy loss processes of energetic electrons and protons as they move out from the central SB source region into the outer galactic disk.

Measurements of very-high-energy (VHE: ≥ 100 GeV) emission from NGC 253 have so far resulted only in an upper limit obtained from observations with the H.E.S.S. (Aharonian et al. 2005) Cherenkov telescopes. This limit is close to previous estimates of the HE γ -ray emission from this galaxy (Goldshmidt & Rephaeli 1995, Romero & Torres 2003, Domingo-Santamaria & Torres 2005). The latter authors calculated HE γ -ray emission from the SB region of NGC 253 based solely on spectral description of the electron and proton distributions. Thus, on both observational and theoretical grounds, and the additional motivation provided by improved observational capabilities afforded

* E-mail: yoelr@wise.tau.ac.il

by the expected upgrade of Cherenkov telescopes, there is considerable interest in a more realistic treatment of the full nonthermal (NT) emission from NGC 253. Moreover, recent detailed radio measurements of this galaxy (Heesen et al. 2008) clearly show the spatial distribution of the emission and its spectral index in the central region, disk, halo, providing an improved observational basis upon which the spectral and spatial distributions of the radio emitting electrons can be determined more precisely than was previously possible. These considerations spur our renewed interest in a substantially more detailed description of the electron and proton populations and their radiative yields.

Our main goal in the work reported here is obtaining an estimate of the HE flux of NGC 253, more reliably than can be obtained by the traditional, very approximate approach, in which the electron energy spectrum is determined from the observed radio flux, and the proton spectrum is then deduced by using an overall scaling of the proton to electron ratio, which in turn is used to estimate the high energy emission from π^0 decay (following the production of the pions in energetic proton interactions with protons in the gas). However, in this simplified approach the electron spectrum needs to be extrapolated to energies much higher than the $\sim 1 - 10$ GeV range directly inferred from radio measurements; therefore, a realistic estimate of the VHE emission requires a more detailed and extensive treatment. For this purpose we use a numerical code which evolves an initial particle source spectrum in the SB acceleration region by following all the relevant leptonic and hadronic interactions as the particles diffuse and convect to the outer disk (and halo). In the first application of this code we calculated the γ -ray spectrum of the nearby SBG M 82 (Persic, Rephaeli, & Arieli 2008: hereafter PRA). A comparison of the predicted spectrum with the predictions from approximate treatments (previous as well as our own) clearly demonstrates the need for a detailed numerical calculation.

This paper presents only the most essential aspects of our treatment; to avoid unnecessary repetition we do not repeat here full details of the basic approach which can be found in PRA. In Section 2 we briefly summarize the main aspects of our treatment of the evolution of energetic electron and proton spectro-spatial distributions as the particles diffuse and convect out of their acceleration sources in the central SB region. Input conditions in NGC 253 are specified in Section 3, together with the steady state spectra and VHE fluxes as calculated numerically using our code. We end with a brief discussion in Section 4.

2 STEADY-STATE TREATMENT

High-mass stars form at a rate that is much higher in the central SB region than in the rest of the galactic disk. Because of this we may simplify the treatment by assuming that direct particle acceleration is limited to the central SB region, which we refer to as the source region. Acceleration in SN shocks by the first-order Fermi process yields a power-law distribution with index $q=2$ (e.g., Protheroe & Clay 2004) in a very wide energy range, from a value close to the mean thermal energy of the gas particles (in non-relativistic shocks) to a very high value ($\geq 10^{14}$ eV). The accelerated proton-to-electron (p/e) density ratio, N_p/N_e , in the source region can be calculated assuming charge neutrality (Bell 1978, Schlickeiser 2002). This ratio reaches its maximum value, $(m_p/m_e)^{(q-1)/2}$ (for $q>1$), over most of the range of particle energies; m_e and m_p are the electron and proton masses. For the full dependence of this ratio on particle energy, and more discussion on this and other relevant physical processes, see PRA and references therein.

The theoretically predicted value of the density ratio is valid in the source region, where energy equipartition is more likely to be attained since the relevant processes couple particles and fields more effectively than over the whole galactic disk. We thus infer N_p in the source region from N_e , which in turn is deduced from radio measurements in the central SB region. Specifically, by adopting the theoretically expected expression $N_p/N_e = (m_p/m_e)^{(q-1)/2}$ in the SB source region, we compute N_p from the electron density, which is itself determined from a comparison of the predicted radio spectrum with the observed spectrum. The fit provides both the normalization of the electron spectrum and the *actual* value of q , which is found to be larger than 2 even in the central SB region. In this procedure the electron population is composed of both primary and secondary electrons, with the latter self-consistently determined by accounting for the pion yield of energetic protons with protons in the gas. A similar procedure was implemented in our similar numerical treatment in PRA.¹

As the particles move out of the acceleration region their respective energy distributions ('spectra') will evolve differently due to their different energy loss processes. The electron spectrum is more easily measured than that of protons due to their more efficient radiative losses, with electron synchrotron radio emission typically the most precisely measured. The electron spectrum can be inferred in the region where the radio emission is observed. This quantity can be related to the source spectrum through a solution of the kinetic equation describing the propagation mode and energy losses by electrons as they move out from their SN shock regions. The proton spectrum can then be determined based on the predicted N_p/N_e ratio at their common source region.

Strictly speaking, we assume that steady state is attained and proceed to solve the kinetic equation for $N_i(\gamma, R, z)$, where $i = e, p$; γ is the Lorentz factor, and R and z are the 2D spatial radius and the coordinate perpendicular to the galactic plane, respectively. Calculations of the particle steady-state spectra necessitate inclusion of all the important energy loss mechanisms and modes of propagation; to do so we have employed the numerical code of Arieli & Rephaeli (in preparation), which is based on a modified version of the GALPROP code (Moskalenko & Strong 1998, Moskalenko et al. 2003). The code solves the exact Fokker-Planck transport diffusion-convection equation (e.g., Lerche & Schlickeiser 1982) in 3D with given source distribution and boundary conditions for electrons and protons. Evolution of particle energy and spatial distribution functions is based on diffusion, and convection in a galactic wind.

At high energies the dominant energy losses of electrons are synchrotron emission and Compton scattering by the FIR and optical

¹ Note that in their description of our similar analysis to estimate the VHE emission from M82, de Cea del Pozo, Torres, & Rodriguez-Marrero (2009) state that we used a much higher value for the latter ratio. Neither this nor their claim that we did not properly include secondary electrons are correct.

Table 1. Measured values of NGC 253 parameters.

| Parameter | Value | Units | Reference |
|--------------------------------|--------------------|-------------|-----------|
| Distance | 2.5 | Mpc | 2 |
| SB region radius | 200 | pc | 6,7 |
| SB region height | 150 | pc | 6,7 |
| Disk radius | 10 | kpc | |
| $M_{H2}(R < 1.1 \text{ kpc})$ | 4.8×10^8 | M_{\odot} | 8 |
| $M_H(R < 600 \text{ pc})$ | 4.8×10^8 | M_{\odot} | 2 |
| $M_H(R < 10 \text{ kpc})$ | 2.5×10^9 | M_{\odot} | 1 |
| $M_{HI}(R < 6.35 \text{ kpc})$ | 2×10^7 | M_{\odot} | 5 |
| Dust temperature | 50 (SB), 16 (disk) | K | 3 |
| Dust emissivity index | 1.5 | | 3 |

References to listed data: (1) Boomsma et al. 2005; (2) Bradford et al. 2003; (3) Melo et al. 2002; (4) Sreekumar et al. 1994; (5) Strickland et al. 2002; (6) Timothy et al. 1996; (7) Ulvestad 2000; (8) Canzian et al 1988.

radiation fields. These well known processes need no elaboration; the level of the ensuing emission depends on the mean strength of the magnetic field, B , and the energy density of the radiation fields, which are specified below. At energies below few hundred MeV, electrons lose energy mostly by Coulomb interactions with gas particles, leading to ionization of neutral and charged ions, and electronic excitations in fully ionized gas.

At low energies proton losses are dominated by Coulomb interactions with gas particles. Protons with kinetic energy above pion masses (~ 140 MeV) lose energy mainly through interactions with ambient protons, yielding neutral (π^0) and charged (π^{\pm}) pions. Neutral pions decay into photons, while decays of π^{\pm} result in relativistic e^{\pm} and neutrinos. In our treatment the electron component always includes both primary and secondary electrons; the latter are produced in π^- decay following pion production in pp interactions of accelerated protons with interstellar gas.

To determine the steady state distributions of electrons and protons we need to specify the densities of neutral and ionized gas in the central SB region and throughout the disk, properties of the magnetic fields, and the energy density of the ambient radiation field (in addition to the CMB), particularly in the IR region. Mean observed values of all these quantities are selected from the literature, including - when available - some knowledge of their spatial variation across the disk. Parameter values are listed in Table 1; observational uncertainties are taken into account in our estimation of the integrated VHE flux. As discussed in PRA, we assume magnetic flux conservation in the ionized gas, and accordingly relate the mean strength of the field to the local plasma density, n_e , using the scaling $B \propto n_e^{2/3}$ (e.g., Rephaeli 1988). The power-law index is only somewhat lower (1/2) if instead energy equipartition is assumed and the magnetic energy density is scaled to the thermal gas energy density. We adopt the ionized gas density profile, $n_e \propto \exp(-z/z_0)/(1 + (R/R_0)^2)$, with $R_0 = 1.5$ kpc, and $z_0 = 0.5$ kpc (Strickland et al. 2002).

To fully determine particle spectra and the magnetic field strength, we assume energy equipartition in the source region. As noted above, we believe that a minimum energy condition is more likely to lead to equipartition in the central SB region than in the rest of the galaxy. Due to the implicit dependences in the expression for the synchrotron flux, this condition is implemented iteratively to solve for N_e , N_p , and the field strength at the center, B_0 . The particles are assumed to be convected out of their sources by the observed wind with a typical velocity of $\sim 500 \text{ km s}^{-1}$ (Strickland et al. 1997) in the source region. In accord with Galactic cosmic-ray MHD wind models, we assume that the convection velocity increases linearly with distance from the disk plane (e.g. Zirakashvili et al. 1996). A central value of $3 \times 10^{28} \text{ cm}^2/\text{s}$ is adopted for the diffusion coefficient, and its energy dependence is approximated as a power-law with index of 0.5.

For brevity (and to avoid unnecessary repetition), other aspects of our approach are not presented here; these are fully specified in our previous similar treatment of VHE emission from M 82 (PRA). In Table 1 we list the values of all the quantities needed to carry out the full calculation of the steady-state particle spectra and the predicted radiative yields.

3 PARTICLE AND RADIATION SPECTRA

Radio emission from the disk of NGC 253 was observed at several frequencies by Klein et al. (1983); additional medium resolution measurements of the SB region were made by Carilli (1996). Detailed, higher resolution mapping of emission from the disk and inner halo of NGC 253 was recently carried out by Heesen et al. (2008) based on new VLA observations at 6.2 cm, Effelsberg observations at 3.6 cm, and previous VLA measurements at 20 and 90 cm. We normalize the electron source spectrum based on the measured radio flux from the SB region (Carilli 1996), and determine some of our best-fit parameters by comparing our predicted radio emission from the galactic disk with the spectrum measured by Heesen et al. (2008).

Fitting the predicted synchrotron radio spectrum to the radio measurements provides the critical normalization of the steady state electron and - based on theoretical prediction - proton energy distributions. Inclusion of all the relevant processes - Coulomb, synchrotron and Compton - is *essential* for precise normalization. Measured radio fluxes from the SB (Klein et al. 1983) and disk (Heesen et al. 2008) regions are shown in Figure 1, together with our best fit spectra. The fact that the predicted radio spectrum is not a single power-law but

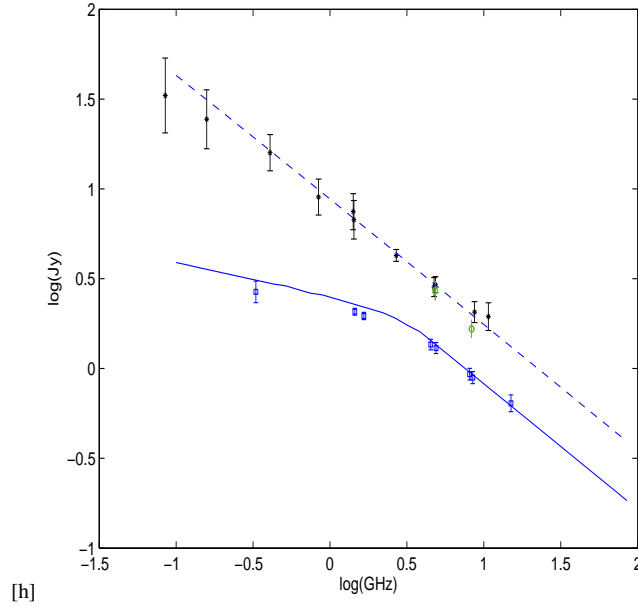


Figure 1. Radio measurements of the SB and entire disk regions of NGC 253. The solid line is our fit to the emission from the SB region; the dashed line is a fit to the emission from the entire disk. Data are from Klein et al. (1983, black dots), Carilli (1996, blue squares), and Heesen et al. (2008, green circles).

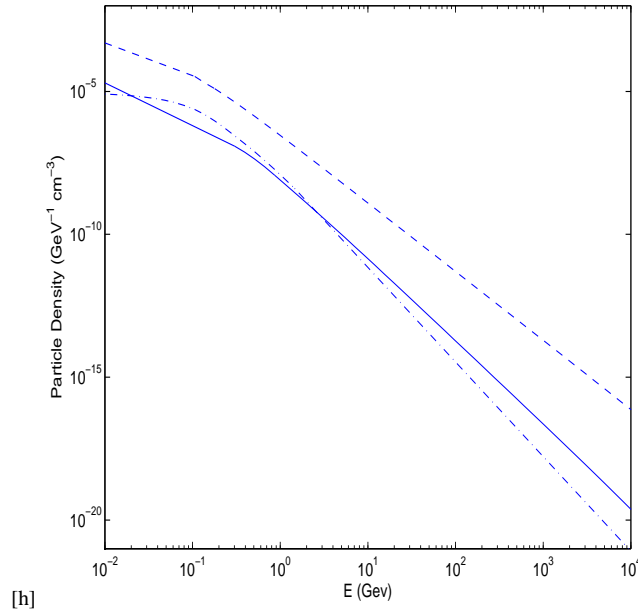


Figure 2. Steady state primary proton (dashed line), primary electron (solid line), and secondary electron (dashed-dotted line) spectral density distributions in the central SB region NGC 253.

curves at sufficiently low frequencies is due to the dominance of Coulomb losses over the other two mechanisms at low electron energies. For the specific combination of values of the field and gas density (which we have deduced from observations), the curvature is particularly pronounced (at around ~ 3 GHz) in the source region. This expected behavior is a diagnostically important feature confirming the self-consistency of our approach. The fit to the radio measurements from the full disk yields a mean radio index $\alpha = 0.7 \pm 0.05$.

As noted above, energy equipartition was assumed and implemented iteratively to solve for N_e , N_p , and B_0 . Doing so we obtain the central value of the magnetic field, $B_0 \simeq 190 \pm 10 \mu\text{G}$. The corresponding steady-state electron and proton spectra in the SB region are shown in Fig.2. At low energies the spectra are appreciably flatter than at high energies. Stronger electron losses at $E \gg 1$ GeV result in a steeper spectrum than that of protons, with the electron spectrum characterized by $q \simeq 2.74$ at high energies, as compared to $q \simeq 2.55$ for protons. We note that the validity of the usual equipartition relation between particle and field energy densities has been questioned (e.g., Beck & Krause 2005), but in our case the revised relation proposed in the latter paper would hardly affect the deduced mean field value.

Our main interest here is the estimation of the total emission at high γ -ray energies. In Fig. 3 we plot electron bremsstrahlung and

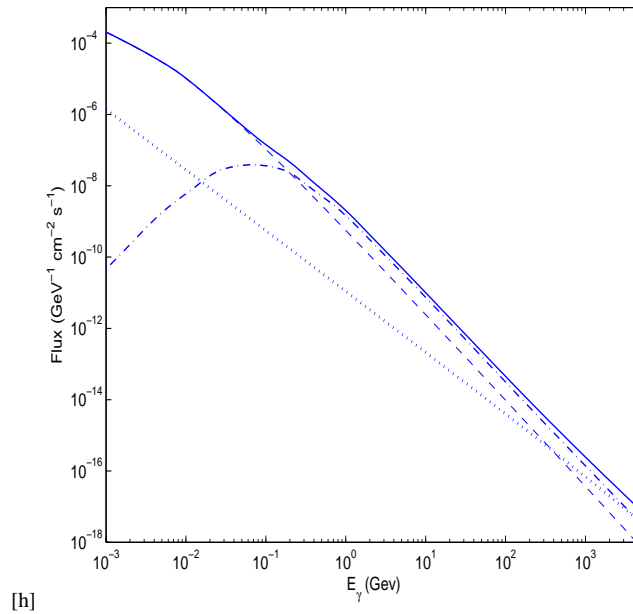


Figure 3. Spectra of high-energy emission processes in the disk region of NGC 253. Radiative yields are from electron Compton scattering off the FIR radiation field (dotted line), electron bremsstrahlung off ambient protons (dashed line), π^0 decay (dashed-dotted line), and their sum (solid line).

Compton spectra, and γ -ray emission from the decay of π^0 formed in p-p collisions. As anticipated, the losses due to bremsstrahlung dominate at low energies, while emission from π^0 decay dominates at higher energies. (Synchrotron emission is negligible at high energies.)

The integrated flux from the disk of NGC 253 is shown in Fig. 4 by the grey region; the width of this region reflects uncertainties in the values of the main observationally-deduced parameters. The total flux above 100 GeV is $f(\geq 100 \text{ GeV}) \simeq (3.6^{+3.4}_{-1.7}) \times 10^{-12} \text{ cm}^{-2} \text{ s}^{-1}$, for $B_0 \simeq 190 \pm 10 \mu\text{G}$, the deduced range of the radio index, $\alpha = 0.7 \pm 0.05$, and the uncertainty in the ambient gas density. As expected, VHE emission comes mainly from the hadronic π^0 decay channel. Emission at these energies is mostly from the SB region, with the rest of the disk contributing 20% – 40% of the total emission. The flux at $\epsilon \geq 50 \text{ GeV}$ is a factor of ~ 3.6 higher. Emission at much lower energies can be measured by the currently operational *Fermi* satellite; for example, we predict an integrated flux $f(\geq 100 \text{ MeV}) \simeq (1.8^{+1.5}_{-0.8}) \times 10^{-8} \text{ cm}^{-2} \text{ s}^{-1}$. This value matches the *Large Area Telescope* 5σ sensitivity of this instrument for a 1-yr scanning-mode operation (e.g., Atwood et al. 2009). Of interest is also the related neutrino flux from the decay of charged pions π^\pm (that produce $e^\pm + \nu_e + \bar{\nu}_e + \nu_\mu + \bar{\nu}_\mu$): at $E \geq 100 \text{ GeV}$ the neutrino flux is $\sim 0.3 f(\geq 100 \text{ GeV})$.

Our exact numerical calculation yields flux levels that are lower than those estimated from a semi-quantitative calculation that does not include the full spatial dependences of the magnetic field and particle densities. Details of this approximate treatment are given in our previous paper (PRA) on VHE emission from M 82. As noted there, the two treatments differ most in the description of the particle spatial profiles outside the source region. In the approximate treatment the impact of energy losses and propagation mode of the protons are not explicitly accounted for. This leads to unrealistically high relative contribution of the main disk to VHE emission. Even a slight steepening of the proton spectrum at high energies results in a significantly lower VHE emission.

The TeV fluxes predicted here are below the upper limit set by the H.E.S.S Cherenkov telescope. Treated as a point source, analysis of the H.E.S.S measurements (Aharonian et al. 2005) yielded an upper limit $f(\geq 300 \text{ GeV}) \leq 1.9 \times 10^{-12} \text{ cm}^{-2} \text{ s}^{-1}$ at the 99% confidence level. This limit is higher than the flux predicted here, $f(\geq 300 \text{ GeV}) \simeq (8.9^{+8.1}_{-4.0}) \times 10^{-13} \text{ cm}^{-2} \text{ s}^{-1}$.

4 DISCUSSION

We have performed a detailed calculation of the steady state spectro-spatial distributions of energetic electrons and protons in NGC 253. Our treatment is based on a numerical solution of the diffusion-convection equation, following the particles from their source region throughout the disk as they lose energy and propagate into the interstellar space. A key feature of our treatment is the deduction of the electron spectrum and its normalization in the central region directly from the measured radio emission in the SB region. Adopting the theoretically predicted injection N_p/N_e (which depends on q) in the SB source region, and assuming equipartition to hold in this region, we iteratively derive the electron and proton densities, and the central value of the magnetic field B_0 , by fitting the predicted synchrotron flux to the observed radio spectrum. Doing so fully determines the particle spectra, which are then evolved by solving the diffusion-convection equation to predict the spatial distributions throughout the disk. Consequently, with the assumed spatial profile of the magnetic field set as specified in Section 2, radio emission from the full disk is then fully determined. The fact that the predicted radio spectrum matches well the observed emission from the disk is an important confirmation of the self-consistency of our treatment, and the validity of our assumptions.

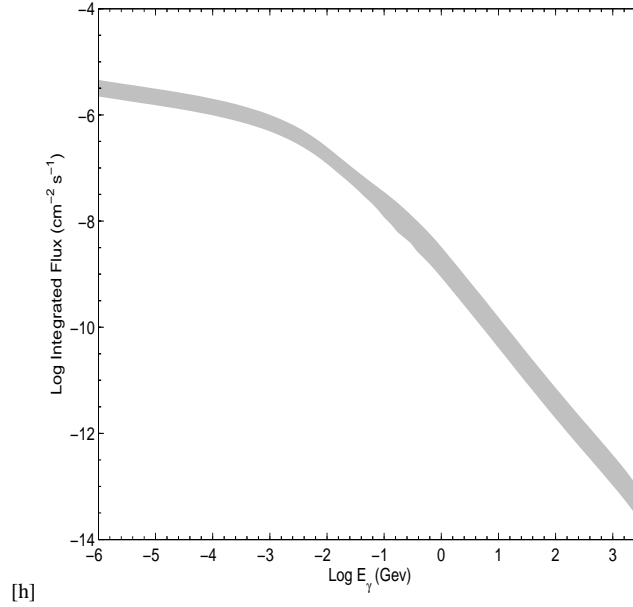


Figure 4. Integrated high energy emission from the disk region of NGC 253. The total integrated emission from the disk region of NGC 253 is shown in the grey region, reflecting uncertainties in the observationally-deduced parameters.

Our main interest here has been the estimation of VHE fluxes from the source region and the entire disk; to do so we determine the particle full radiative spectra, from radio to the VHE region, and use the measured radio fluxes from both regions to normalize the distributions.

HE γ -ray emission from the SB region of NGC 253 was estimated by Domingo-Santamaria & Torres (2005). Their detailed treatment focused on a steady state solution to the kinetic equation describing the electron and proton spectral distribution functions (without explicit spatial dependence). The source term was directly related to SN rates in the injection region, and the particles were assumed to be accelerated by SN shocks in a small central region. Energy losses and diffusion in energy space were followed in the central 1 kpc disk region; escape from this region was also included. Estimated fluxes - which obviously depend on the spectral parameters and the escape time - are generally comparable to our estimates. Our very different treatment includes also spatial diffusion and convection, and our estimates include the full disk, not just the central 1 kpc region. While VHE emission is mostly from the central disk, emission from the outer disk is not negligible and provides additional insight on the validity of the convection-diffusion model for energetic particle propagation in galaxies.

Clearly, our predicted fluxes depend on several parameters, most importantly on the proton to electron ratio in the source region, on the magnetic field, gas density, and their spatial profiles. The electron density was deduced from the measured radio emission in the source region; thus, the evolution of the electron spectrum from this region to the central disk region is mostly determined by synchrotron losses in the high magnetic field. The uncertainty in the estimated level of VHE emission stems largely from the steep dependence of the electron density on the field. It is unlikely that the field is appreciably higher than our deduced value, $B_0 \sim 200 \mu\text{G}$. A lower mean field value (by a factor ζ), would result in a reduced proton density and, consequently, in a lower rate of π^0 decays. However, for a given measured radio flux the electron density would have to be correspondingly higher (by a factor $\zeta^{(1+q)/2}$), which for a mean electron index of ~ 2.7 (in the disk) would result in higher bremsstrahlung and Compton yields by nearly the same factor ($\sim \zeta^2$). As can be seen in Figure 3, at ~ 100 GeV the yield from the latter processes is only a factor ~ 2.5 lower than emission from π^0 decay. Thus, lowering the mean field value in the source region by even as much as a factor of two (i.e., much higher than the uncertainty implied from the observational radio flux data) would not appreciably change our estimated VHE fluxes. The other main uncertainty stems from the linear dependence of the p-p interactions (and π^0 decay yield) on the ambient proton density, for which we used the observationally deduced mass in the central disk region.

The range of predicted fluxes, which reflect observational uncertainties in these quantities, provide a basis for reliable estimates of the feasibility of detecting VHE emission from NGC 253 with current and near future telescope arrays, and detection of HE γ -ray emission with GLAST. Based on the above estimate, the predicted VHE flux of NGC 253 falls below the detection limit of current imaging air Cherenkov telescopes (IACTs). For example, H.E.S.S. - which is located in the Southern hemisphere and can therefore observe NGC 253 - has a 5σ sensitivity of $\sim 1.8 \times 10^{-11} \text{ cm}^{-2} \text{ s}^{-1}$ for the detection of emission above 100 GeV in 50 hours of observation (e.g., Hinton 2004). Even accounting for the fact that this sensitivity limit refers to a Crab-like spectrum [which is steeper ($\Gamma \simeq 2.6$) than our predicted NGC 253 spectrum], and for the inherent uncertainty in our flux estimate, we conclude that detection of VHE γ -ray emission from NGC 253 may be feasible with H.E.S.S. only if observed for several hundred hours. [Prospects of detection with CANGAROO III are even less optimistic due to its lower sensitivity by a factor 3-5 (Enomoto et al. 2008).] The likelihood of detection will appreciably improve with the upcoming H.E.S.S.-II telescope, whose sensitivity at ≥ 100 GeV is expected to be $\lesssim 0.6 \times 10^{-11} \text{ cm}^{-2} \text{ s}^{-1}$, i.e. ~ 3 times better than H.E.S.S., and with

the next-generation facility (the Cherenkov Telescope Array, CTA) whose sensitivity at ≥ 100 GeV is expected to be $\lesssim 10^{-12}$ cm $^{-2}$ s $^{-1}$, i.e. at least $\gtrsim 20$ times better than H.E.S.S.

It is also of interest to compare the predicted ≥ 100 MeV flux of NGC 253 with the sensitivity of *Fermi*'s Large Area Telescope (LAT). Our calculated VHE emission yields an integrated flux $f(\geq 100 \text{ MeV}) \simeq 2 \times 10^{-8}$ cm $^{-2}$ s $^{-1}$ for a differential spectral photon index of ~ 2.3 . This value matches the 5σ sensitivity of the *LAT* for a ~ 1 -month scanning-mode operation. Thus, *Fermi/LAT* should be largely able to detect NGC 253 during its first year of operation.

Detection of VHE γ -ray emission associated with ongoing star formation in NGC 253 will add significant insight on the enhanced energetic electron and proton contents in SBGs, and on their propagation in disks of spiral galaxies.

5 ACKNOWLEDGMENT

We thank the referee for a critical review of the originally submitted version of this paper.

References

- Aharonian, F.A., et al. 2005, *A&A*, 442, 177
 Atwood, W.B., et al. 2009, *ApJ*, 697, 1071
 Beck, R., & Krause, M. 2005, *Astron. Nachr.*, 326, 414
 Bell, A.R. 1978, *MNRAS*, 182, 443
 Boomsma et al. 2005, *ASPC* 331, 247
 Bradford et al. 2003, *ApJ* 586, 891
 Canzian et al 1988, *ApJ* 333, 157
 Carilli C.L. 1996, *ã305*, 402
 De Angelis, A., Mansutti, O., & Persic, M. 2008, *Nuovo Cimento*, 31, no.4, 187
 de Cea del Pozo, E., Torres, D., & Rodriguez Marrero, A. 2009, arXiv:0901.2688
 Domingo-Santamaría, E., & Torres, D.F. 2005, *A&A*, 444, 403
 Enomoto, R., et al. 2008, *ApJ*, 683, 383
 Goldshmidt, O., & Rephaeli, Y. 1995, *ApJ*, 444, 113
 Heesen, V., Beck, R., Krause, M., Dettmar, R.J. 2008, *A&A*, 494, 563
 Hinton, J. 2004, *New Astron. Rev.*, 48, 331
 Klein U. et al. 1983, *ã127*, 177
 Lerche, I., & Schlickeiser, R. 1982, *MNRAS*, 201, 1041
 Melo et al. 2002, *ApJ* 574, 709
 Moskalenko I.V, & Strong A.W. 1998, *ApJ*, 493, 694
 Moskalenko I.V, Jones, F.C., Mashnik, S.G., Ptuskin, V.S., & Strong, A.W., 2003, *ICRC*, 4, 1925
 Persic, M., Rephaeli, Y., & Arieli, Y. 2008, *A&A*, 486, 143 (PRA)
 Protheroe, R.J., & Clay, R.W. 2004, *PASA*, 21, 1
 Rephaeli, Y. 1988, *Comm. Ap.*, 12, 265
 Romero, G.E., & Torres, D.F. 2003, *ApJ*, 586, 33
 Schlickeiser, R. 2002, *Cosmic Ray Astrophysics* (Berlin: Springer), p.472
 Sreekumar et al. 1994, *ApJ* 426, 105
 Strickland et al. 2002, *ApJ* 568, 689
 Strickland, D.K., Ponman, T.J., & Stevens, I.R. 1997, *A&A*, 320, 378
 Timothy et al. 1996, *ApJ* 460, 295
 Ulvestad 2000, *Astron. J.* 120, 278
 Zirakashvili, V.N., Breitschwerdt, D., Ptuskin, V.S., & Voelk, H.J. 1996, *A&A*, 311, 113